Case Studies in Chemical and Environmental Engineering 4 (2021) 100137

Contents lists available at ScienceDirect

Case Studies in Chemical and Environmental Engineering

journal homepage: www.sciencedirect.com/journal/case-studies-in-chemical-and-environmental-engineering

Preparation and modification of low-fouling ultrafiltration membranes for cheese whey treatment by membrane bioreactor

Nasim Bazrafshan [a], Mostafa Dadashi Firouzjaei [b,*], Mark Elliott [b,**], Amitis Moradkhani [c], Ahmad Rahimpour [a,d,***]

[a] Department of Chemical Engineering, Babol Noushirvani University of Technology, Shariati Avenue, Babol Mazandaran, 4714871167, Iran
[b] Department of Civil, Environmental and Construction Engineering, University of Alabama, Tuscaloosa, AL, 35487, USA
[c] Indian Springs School, Pelham, AL, 35124, USA
[d] Department of Mechanical Engineering, Advanced Water Research Laboratory, University of Alberta, Canada

ARTICLE INFO

Keywords:
Membrane bioreactor
Cheese whey wastewater treatment
Metal-organic framework
Environmental chemical engineering

ABSTRACT

This case studied the treatment of cheese whey wastewater (CWW) from the Kalleh® dairy industry using a membrane bioreactor (MBR). The coagulation process and activated sludge sections eliminated 26% and 75% of organic matter from CWW with chemical oxygen demand (COD) of 10,000 mg/l, respectively. In the MBR, metal-organic framework (MOF)-modified PSf membranes enhanced the whole system's performance. The flux of water and CWW increased from 157 and 28 (L/m^2.h) to 350 and 60 (L/m^2.h), respectively, by only 2 wt% MOF concentration. The reduction of COD in the overall system was around 98.8%.

1. Introduction

Wastewaters of food processing facilities typically have much higher chemical oxygen demand (COD) and biological oxygen demand (BOD) than other industries or municipalities [1,2]. The dairy industry produces especially large volumes of high-strength wastewater where CWW contain high organic matter, mineral salts, total suspended solids (TSS), nutrients, oils and fats, acidity, salinity, etc. [3,4]. As a byproduct of the cheese manufacturing process, Cheese whey has a high organic content [5]. Cheese whey wastewater (CWW) with high COD (800–77,000 ppm) and BOD (600–16,000 ppm) gets disposed to the wastewater [6,7]. One of the most critical challenges for CWW treatment is to use a cost-efficient and suitable way to recycle the water [8,9].

Aerobic and anaerobic treatments are the main methods for CWWs remediation, which usually includes biological (e.g., activated sludge (AS)) processes, aerated lagoons, sequencing batch reactor (SBR), trickling filters, up-flow anaerobic sludge blanket reactor, and anaerobic filters [10,11]. However, these treatment techniques have problems that lead to either common operational difficulties or high energy requirements [12]. Undoubtedly, the Membrane process is considered one of the most efficient methods for water and industrial effluents treatment [13,14]. Being simple to scale up with high performance and easiness in construction made this technology a fundamental water and wastewater treatment component [15]. Also, this way can be used to recover significant compounds like protein and lactose in a cheap method as an economic origin that can be applied in food, dairy, and pharmaceutical industries [16,17]. In addition, membrane technology is a safe way to solve the environmental pollution issues by removal a high percent of organic and hazardous materials from CWW [18]. The most favorable applied membrane in cheese whey wastewater treatment is the ultrafiltration membrane [1,19–21]. Recently, researchers have begun to investigate the treatment of CWW through membrane-based processes due to considerable gains in reliability and cost efficiency [22,23]. There is a growing fondness for combining the biological treatment of CWW with membrane processes because of the increase in wastewater treatment costs and environmental pollution by polluted dairy effluent.

Membrane bioreactor (MBR) is one of the most convenient and facile separation processes for CWW and has attracted substantial attention [24]. When supplemented with additional treatment steps (e.g., by coagulation, electrochemical treatment, adsorption), a treatment featuring MBR can yield nearly complete removal of organic matter

* Corresponding author.
** Corresponding author.
*** Corresponding author. Department of Civil, Environmental and Construction Engineering, University of Alabama, Tuscaloosa, AL, 35487, USA.
E-mail addresses: mdfirouzjaei@crimson.ua.edu (M. Dadashi Firouzjaei), melliott@eng.ua.edu (M. Elliott), ahmadrahimpour@nit.ac.ir (A. Rahimpour).

https://doi.org/10.1016/j.cscee.2021.100137
Received 18 August 2021; Received in revised form 19 September 2021; Accepted 23 September 2021
Available online 25 September 2021

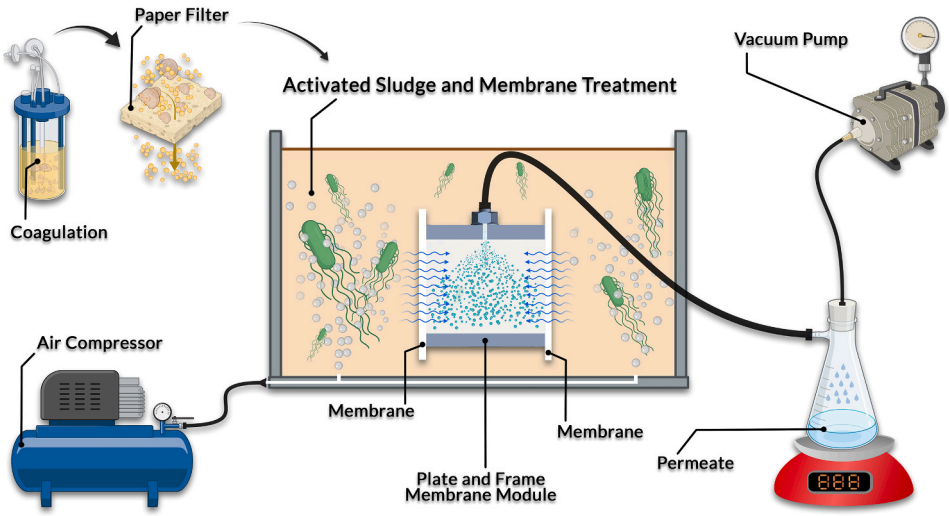

Fig. 1. The graphical representation of the MBR treatment system.

from CWW [25,26]. A unique advantage of the MBR process relative to other CWW treatment technologies is the capacity of membranes for the complete retention of all microorganisms. Moreover, high-quality effluent, independence of hydraulic retention time (HRT), higher solids retention time (SRT), and easy control are MBR's main advantages over chemical-based processes [27,28]. However, various types of fouling like colloidal fouling, organic fouling, and microbiological fouling, which increase operation costs, are still the main problems that limit the widespread use of MBR [29,30]. In addition, biofouling resulting from AS composition can severely affect the membrane surface physics [31–33]. Accordingly, many studies have investigated ways to prevent fouling, like modifying membrane surface chemistry [34], optimization of biomass characteristics [35], and correction of operating conditions [36]. Several investigations have been reported on adding porous and functional nanoparticles in the casting solution to achieve higher performances from the membrane with considerable antifouling improvements [37,38]. The most common nanoparticles that have been used to improve the membrane antifouling activity are titanium dioxide (TiO_2) [39–42], alumina (Al_2O_3) [43–45], Zirconium dioxide (ZrO_2) [46], zinc oxide (ZnO) [47,48], carbon nanotubes [49], silicon dioxide (SiO_2) [50–52], zeolites [53], and polyaniline (PANi) nanomaterials [54,55]. However, the poor dispersion of the nanoparticles in the polymer matrix might result in poor selectivity of the mixed matrix membranes [56,57].

Metal-organic frameworks (MOFs) are hybrid organic-inorganic crystalline materials that consist of metal ions or metal ion clusters linked by organic ligands to form a coordinated structure [58–60]. The main advantages of mixed-matrix MOF-membranes are creating selective cavities and increasing permeability and porosity [61,62]. Echaide et al. [63] showed that using ZIF-11 MOF nanoparticles in the fabrication of thin-film polyamide membranes led to increased porosity, hydrophobicity, and rejection.

In this study, the efficacy of the MOF on the performance and morphology of PSf UF membranes for CWW treatment has been studied. Performance of modified membranes was tested in terms of the water flux, cheese whey wastewater flux (CWW), natural organic matters (NOM) removal, and chemical oxygen demand (COD) removal of the CWW. Finally, the CWW was treated by submerging the MOF-modified polysulfone (PSf) membrane in the MBR for 8 days. MOF nanoparticles created a highly porous and hydrophilic structure mixed-matrix membranes, resulting in enhanced antifouling properties COD removal. Based on the authors' knowledge, this is the first report on applying copper-based MOF in MBR.

2. Experimental

2.1. Materials

Udel P3500 PSf beads (Solvay polymers) were utilized as a polymer matrix for membrane fabrication. Polyethyleneglycol, 600 Da ((PEG) as the pore former, 99.5% N-Methyl-2-pyrrolidone (NMP) as an organic solvent, and Triton X-100 were all bought from Merck, Germany company. Acidic cheese whey with pH = 5.5 ± 0.5 and COD = 73,000 mg/L as the dairy feed and AS were collected from the dairy plant of Kalleh® Company, Amol, Iran. The whey sample was kept at 3 °C to avoid changes in chemical composition and acidification. Furthermore, $FeCl_3$ solution was consumed for the coagulation process.

2.2. MBR system

Fig. 1 reveals the schematic graphic of the MBR system used in this study. The integrated batch process for advanced treatment of the cheese whey consists of physicochemical pre-treatment and in-situ biological membrane unit as a post-treatment.

2.3. Coagulation and precipitation process

Due to the large volume of suspended solids in the influent, coagulation was used to isolate and remove these solids. First, raw CWW was diluted with deionized (DI) water (with the ratio of 1:9) to reduce the COD to 10000 mg/l. $FeCl_3$ aqueous solution with the concentration of 160 mg/L was added to the diluted solution and stirred at the speed of 150 rpm for 2 minutes. The flocculation process was performed for 20 minutes at a rate of 20 rpm. Then, the solution was rested for an hour to precipitate the coagulated particles. Finally, NaOH solution was used to neutralize the pH (7–8).

2.4. Synthesis of copper MOF

Copper MOF (CuMOF) was synthesized according to the method described elsewhere [64]. Briefly, copper (II) nitrate trihydrate (1.5 g) and 1, 3, 5-benzenetricarboxylic acid (1 g, H3BTC) was added in 200 mL of dimethylformamide (DMF) as a solvent, and the mixture was sonicated for 30 min in an ultrasonic bath. Then to complete the reaction, the solution was heated at 80 °C for 12 h. Then, the mixture cooled down to the ambient temperature and washed twice with a DMF solvent. The precipitates were dried in the oven at 80 °C for 8 h. In the final step, the synthesized CuMOF was dried for 12 h at 120 °C to remove moisture and

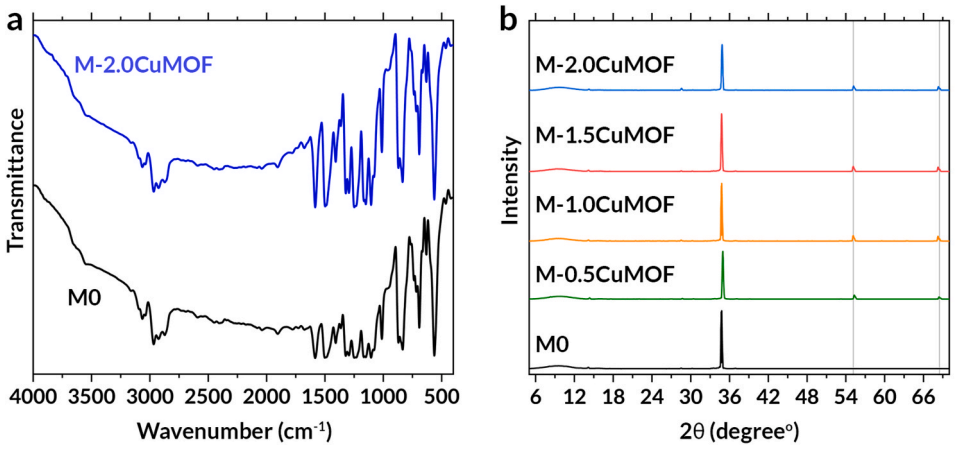

Fig. 2. (a) FTIR-ATR spectra and (b) XRD results of the neat and modified membrane.

solvent.

2.5. Membrane preparation and modification

The neat and mixed-matrix ultrafiltration PSf membranes were prepared by the conventional NIPS method [65]. The neat membrane was fabricated by the addition of the PSf beads (16 wt%) to a mixture containing Triton X-100 (1 wt%) as the surfactant, PEG (2 wt%) as a pore-forming agent, and NMP as solvent. To prepare PSf mixed-matrix membranes, using an ultrasonic bath for 1 h, various amounts of CuMOFs (0.5, 1, 1.5, and 2 wt%) were dispersed in NMP. Then, 2 wt% of PEG, 16 wt% of PSf, and 1 wt% of Triton x-100 were mixed with CuMOF mixture and was stirred at 200 rpm for 24 h. After sonication, the mixture rested for 60 min to remove the entrapped air bubbles. Finally, the 100 μm thick membranes were casted on non-woven polyester and immersed in a coagulation bath (0.1 wt% sodium dodecyl sulfate). Finally, the flat sheet membranes were kept in pure freshwater to remove any residual solvent. According to the concentration of MOF used in the casting solution, the synthesized membranes were labeled as M − 0, M-0.5CuMOF, M-1CuMOF, M-1.5CuMOF, and M-2CuMOF in which numbers denote the content of MOFs.

2.6. Membrane characterization

The cross-section and surface of the membranes were evaluated by field emission scanning electron microscope (FESEM) coupled (Apreo, Thermo Scientific). The roughness and surface morphology of the membranes were characterized by atomic force microscopy (AFM, Easyscan2 Flex). X-ray diffraction (XRD, Bruker D8, Germany) spectra of neat and MOF modified membranes were tested with Cu Kα radiation.

The water contact angle (CA) measurement (G10, KRUSS, and Germany) was used to evaluate the hydrophilicity of the membrane surfaces. The Fourier transform infrared (FTIR) spectroscopy analyzed the surface chemistry of the membranes. The membranes' porosity was measured by Equation (1).

$$\varepsilon\ (\%) = \frac{(m_{wet} - m_{dry})/\rho_w}{\frac{m_{wet}-m_{dry}}{\rho_w} + \left(\frac{m_{dry}}{\rho_p}\right)} \quad (1)$$

where Ɛ % is membrane porosity, ρ_p is the polymer density, and ρ_w is the water density, m_{wet}, and m_{dry} are the wet and dry masses of membranes, respectively.

2.7. Membrane filtration performance

The fabricated membranes' separation properties were measured using a dead-end stirred cell with an effective membrane area of 20 cm^2. The membranes were compacted for 1 h at a pressure of 3 bar before the filtration experiments using pure water. The water flux has been calculated as follows:

$$J_w = \frac{V}{A.\Delta T} \quad (2)$$

where V (L) is the volume of permeated water, J_w ($L/m^2.h$) is the pure water flux, ΔT (h) is the permeation time, and (m^2) is the effective area of the sample.

The filtration performance of the membranes was investigated in terms of COD and natural organic matter (NOM) removal using cheese whey as feed at 3 bar. The COD and NOM of permeate were measured using an ultraviolet-visible spectroscopy spectrophotometer (Chrom Tech, USA) at 254nm and spectrophotometer (Aqualytic, model ET-108, Germany), respectively. The membranes performance was determined as follow:

$$R(\%) = \left(1 - \frac{C_P}{C_f}\right) \times 100 \quad (3)$$

where C_p and C_f are permeate and feed concentration, respectively. In case of flux and rejection, the average value of three separate membranes was reported to minimize the experimental error. Statistical analysis, including a *t*-test with two-tailed distribution with significant differences (P-value) of $\alpha = 0.05$, was conducted to approve precise data measurement. Microsoft Excel software was used to adopt calculation, in which P values of less than 0.05 offer the differences are statistically significant.

2.8. Evaluation of antifouling properties

For antifouling tests, membranes were first compacted by pure water filtration at 3 bar for 2 h. Then, the membrane's pure water flux (PWF) was collected for 30 min ($J_{pw,1}$). Then, CWW was fed to the ultrafiltration system, and the flux, J_{CWW}, was obtained for 2 h. Afterward, the fouled membranes were cleaned with distilled water for 40 min. Finally, for 30 mins, the PWF was measured again ($J_{pw,2}$). The irreversible fouling ratio (R_{ir}), reversible fouling ratio (R_r), flux recovery ratio (FRR), and total fouling ratio (R_t) were calculated as follow:

$$\mathrm{FRR}(\%) = \frac{Jpw,2}{Jpw,1} \times 100 \quad (4)$$

$$\mathrm{R_r}(\%) = \frac{Jpw,2 - Jcww}{Jpw,1} \times 100 \quad (5)$$

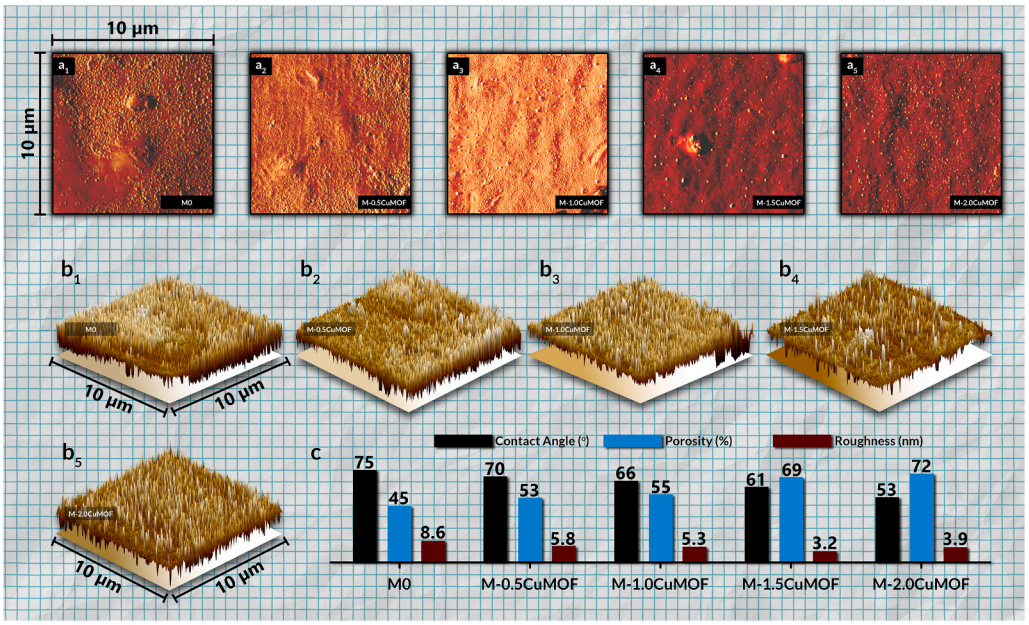

Fig. 3. The AFM and CA results of the modified and unmodified membranes; a_1,b_1) the AFM of M0; a_2,b_2) the AFM of M0.5; a_3,b_3) the AFM of M1; a_4,b_4) the AFM of M1.5; a_5,b_5) the AFM of M2; c) the CA, porosity, and roughness of membranes.

$$R_{ir}(\%) = \frac{Jpw,1 - Jpw,2}{Jpw,1} \times 100 \quad (6)$$

$$R_t(\%) = \frac{Jpw,1 - Jcww}{Jpw,1} \times 100 \quad (7)$$

Each filtration data is an average of three different experiments to provide an accurate measurement. A comparison of values was reported to calculate the rejection, flux, and antifouling properties of pristine PSf and Cu-MOF/PSf membranes. Finally, the average data was reported to minimize the experimental error.

2.9. Membrane bioreactor process

The membrane with optimized performance and rejection was used

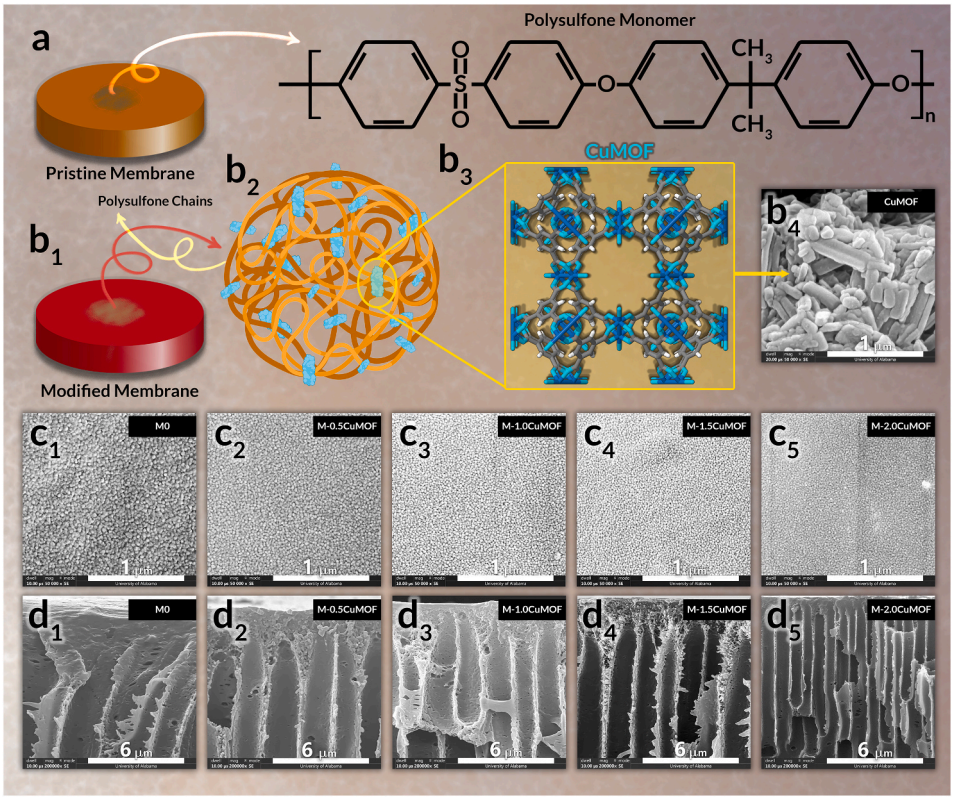

Fig. 4. a) Chemical formula of pristine membrane; b1-b2) schematic design of the modified membrane; b3) 3D structure of the MOF; b4) FESEM image of MOF; c1-c5) FESEM surface images of membranes; d1-d5) Membranes FESEM Cross-sectional images.

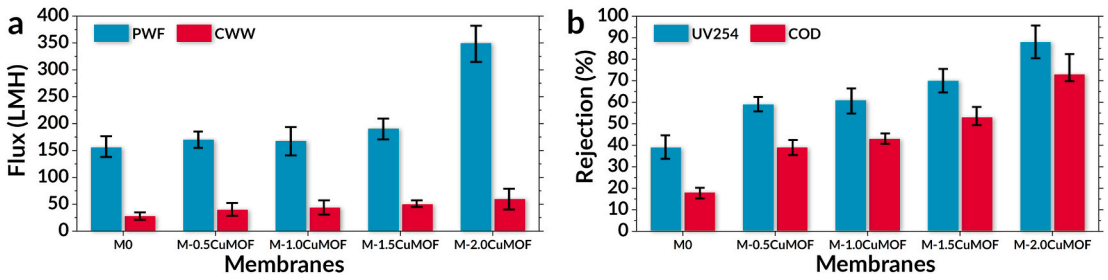

Fig. 5. (a) PWF and CWW flux of the membranes, (b) Rejection of the membranes.

for submerged membrane bioreactors, as shown in Fig. 1. The optimized HRT of 24 h was considered for the activated sludge system. A plate and frame membrane cell with an effective surface area of 0.022 m^2 was submerged in the bioreactor for 8 days. A vacuum pump was used to collect the purified. Each day the CWW feed was added to the system to keep process conditions constant.

3. Results & discussion

3.1. Membranes physiochemical characteristics

Fig. 2a represents the FTIR results of the neat and modified membranes. The bands characterized pristine PSf with asymmetric C–O–C at 1243 cm^{-1}, aromatic C=C stretching at 1584, 1492 cm^{-1}, asymmetric O=S=O stretching at 1151 cm^{-1}, symmetric O=S=O stretching at 1105 cm^{-1}. However C=O symmetric band at 1647 cm^{-1}, C–O at 1369 cm^{-1} dominates PSf low-intensity bands of asymmetric C–O–C stretching at 1243 cm^{-1} and asymmetric O=S=O stretching at 1105 cm^{-1}, confirming the incorporation of CuMOF nanoparticles [66]. The peaks around 1677 cm^{-1} and 1683 cm^{-1} wavenumbers are related to the C=O bond of the carboxylic group of CuMOFs. The extra peak visualized at 2500-3000 cm^{-1} refers to tensile vibrations of the OH group in a modified membrane [52]. Additionally, the hydroxyl group is presented in the peak of 950 cm^{-1}. The appearance of peaks in the range of 1320-1000 cm^{-1} corresponded to the C=O group of carboxylic acid. The tensile vibrations of C-C are evident at the peaks of 996, 1054, and 1105 cm^{-1} wavenumbers [67].

XRD test was performed to detect the crystalline structure of CuMOFs in the PSf matrix, and the spectrums are shown in Fig. 2b. The XRD results of modified membranes demonstrated peaks at 55.1°, 68.0° attributed to the CuMOF [68], while such peaks have not been observed in M0 blank membrane. This confirms the successful addition of CuMOF to the chains of PSf emerging by the ordered crystalline structure of CuMOF [68]. The emergence of new peaks on the XRD and FTIR results of the membranes both support the idea of CuMOF incorporation into the structure of the membrane [69].

Fig. 3 indicates the AFM images and CA results of neat and modified membranes. Fig. 3 shows that the addition of CuMOF to the casting solution decreased membranes' surface roughness. This can be attributed to the rapid phase inversion non-solvent and solvent exchange rate. Furthermore, the agglomeration of CuMOF nanoparticles by increasing their concentration in casting solution affected the membrane surface by increasing the roughness [70,71]. As shown in Fig. 3c, the membranes' porosity was increased by increasing the concentration of CuMOF. The porosity enhancement can be ascribed to the effect of the CuMOFs on the phase inversion (PI) reaction that induces the fabrication of more porous membranes [70]. Also, the residual porous CuMOFs in the membranes could increase the porosity of membranes [37]. Furthermore, the surface mean pore size of membranes declined from 57 to 24 nm with the addition of MOF. This may be because of the effect of CuMOF on PI kinetics of PSf.

The membranes' CA measurements are provided in Fig. 3c. The neat membrane demonstrated the CA of 75°, while the M-2.0CuMOF membranes showed the CA of 53.5°, indicating the most hydrophilic surface. The reduction of CA can be attributed to the existence of hydrophilic carboxylic groups of CuMOFs on the membrane structure [49].

FE-SEM images of membranes are shown in Fig. 4. The cross-sectional SEM images exhibited an asymmetric structure consisting of transport channels at the bottom, a thick porous middle layer, and a selective layer at the top. This structure is formed by rapid phase change caused by the presence of CuMOFs in the casting solution. The overall porosity of the neat membrane was about 47%, while the 2.0-CuMOF membrane had a porosity of 73%. In addition, it seems that membrane pore size decreased by increasing the concentration of CuMOF. These changes in surface pore size and porosity of the membrane are related to the kinetic effect and thermodynamic of CuMOF content on the PI reaction. The affinity of CuMOF particles to water media during PI varies the kinetic and thermodynamic characteristics of the coagulation process. During the precipitation process, this affinity accelerates the exchange speed between solvent and non-solvent. As a result, a porous sub-layer at the bottom and a thin skin layer at the top with wide and long finger-like architecture were formed [62,72,73].

The PWF, CWW flux, NOM, and COD removals were investigated to evaluate the effect of CuMOF on the performance of prepared membranes, and the results are demonstrated in Fig. 5. All experiments were repeated three times and the intermediate data was reported. As can be seen, PWF and CWF increased with increased loading content of CuMOF in the casting solution. The highest flux of PW and CWW was observed in the M-2.0CuMOF membrane, approximately 350 and 60 LMH, respectively. Adding hydrophilic MOF would increase the water penetration rate into the polymer chains during the PI reaction. In contrast, CuMOF ruptures the polymer chains by decreasing the casting solution's thermodynamic stability and reducing the interfacial diffusion between the polymer chains and the solvent, resulting in a growth in the solvent exhaust. This would enhance the non-solvent and solvent exchange rate, leading to higher porosities [74]. In addition, the highly porous structure of CuMOF and the hydrophilic surface of the modified membrane absorb a higher amount of the water molecules and cause higher PWF [75]. All of these considerations lead to higher PWF and CWW for modified membranes than the pristine membrane.

Fig. 5b shows the rejection factors, including COD removal and UV_{254nm} for the neat and modified membranes. COD decreased for the M0 membrane by about 18%, while the COD removal of about 73% was achieved by adding 2 wt% of CuMOF in the casting solution. This can be attributed to the formation of membranes with smaller pore sizes due to the presence of CuMOF in the casting solution [76–78]. Additionally, the adaptability of the polymer and fillers is an efficient parameter in the membrane's selectivity [71]. Because of the attendance of organic linkers in the CuMOF structure, they demonstrate a higher tendency to stick to the polymer and so exclude the constitution of non-selective voids in the membrane structure. Therefore, modified membranes indicated better rejection than pristine membrane.

3.2. Membrane antifouling properties

Adhesion and accumulation of the foulants on the membrane's

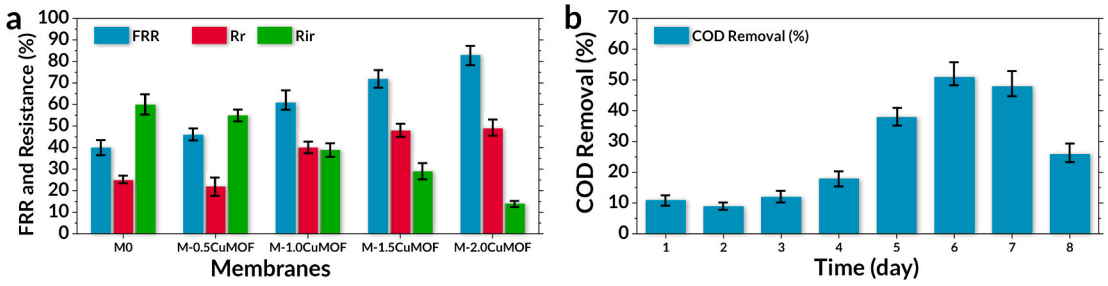

Fig. 6. (a) fouling resistance and flux recovery of membranes (%), (b) COD removal (%) of the membranes in a plate and frame module.

Table 1
Comparison of separation performance of present membranes with literature.

Membrane	PWF Change (%)	Permeate Flux Change (%)	Contact Angle Change (degree)	Contaminant	FRR Increase (%)	Ref
0. 5% Ce-Anth-MOF/PES	+400%	+233%	-20	Humic acid	+100%	[19]
1% salicylate alumoxane/PSf	-13%	+37%	-13	Bovine serum albumin	+37%	[85]
2% TiO2/PSf	+69%	+22%	-43.3	Kerosene	+12%	[86]
0.05% PRh/PSf	93%	+255%	-9.5	Industrial wastewater	+81%	[87]
0.5% Cu-BTC/PES	-46%	–	-12	Milk powder	+237%	[88]
2% CuMOF/PSf	+12%	+114%	-22	Cheese whey	+107%	This work

surface and inside the pores reduce the membrane flux [79,80]. The reversible and irreversible resistance of membranes (R_r and R_{ir}), flux recovery ratio (FRR), and total filtration resistance (R_t) were calculated and presented in Fig. 6a. Membranes' FRR improved with increasing MOF concentration, in which M-2.0CuMOF showed the highest FRR value, showing the better recovery properties of modified membranes and loose adsorption among the surface of the modified membrane and the foulant of the feed solution [81,82]. Moreover, the modified membranes demonstrated lower resistance than the neat membrane, implying lower membrane fouling because of less deposition of foulant [79,80,83].

Similarly, the M-2.0CuMOF had the lowest R_t and R_{ir} values. Hydrophilic particles on the surface and into the pores of modified membranes form a hydration layer on membranes and reduce the interaction between the organic foulants and membrane surface [59]. Furthermore, AFM results agree that the smoother surface will improve the antifouling properties of the membrane [79,80,84].

The M-2.0CuMOF with the best antifouling properties and the highest percentage of COD removal (%) was applied in the bioreactor system to evaluate its performance to treat CWW. The COD of the treated effluent during the 8 days of treatment is provided in Fig. 6b. As it can be seen, the COD of the purified stream decreased steadily until the sixth day, which gives us the maximum decrease on that day. This can be attributed to the saturation of microorganisms and the accumulation of dead microorganisms, colloids, solutes, and cell debris onto the membrane surfaces and/or within the membrane pore spaces because of interactions between the membrane surface and the wastewater.

Finally, a comparison between the M-2.0Cu-MOF membrane in the current study and various PSf and PES modified membranes is provided in Table 1. Some parameters, including membrane type, surface modifying agent and pure water flux, permeate flux, and FRR, are considered to understand better how the CuMOF membranes fabricated in this study indicated considerable advantages over other similar ones previously reported in the literature. Attaining concurrent high COD removal and water and CWW flux are fundamental features for developing a high-performance membrane. In comparison to other membranes, it showed higher water flux and while maintaining higher rejection.

4. Conclusion

In this research, the treatment of CWW was studied by the CuMOF-modified membrane applied in the MBR system. CuMOF-membranes were fabricated by incorporation of CuMOF nanoparticles into the PSf casting solution. Among modified membranes, the M-2.0CuMOF had the best performance in terms of rejection and fouling with organic substances. According to the obtained results, the prepared membrane's PWF and CWW fluxes were reported 350 LMH and 60 LMH, respectively. Moreover, irreversible fouling of 15% was achieved for M-2.0CuMOF. It can be concluded that the addition of CuMOF changed the membrane's morphological structure and pore size. Finally, COD removal of 98% was obtained by M-2.0CuMOF for the whole MBR process.

Declaration of competing interest

The authors declare that they have no known competing financial interests or personal relationships that could have appeared to influence the work reported in this paper.

References

[1] S. Zinadini, et al., Preparation and characterization of antifouling graphene oxide/polyethersulfone ultrafiltration membrane: application in MBR for dairy wastewater treatment, J. Water Process Eng. 7 (2015) 280–294.
[2] D. Orhon, et al., Biological treatability of dairy wastewaters, Water Res. 27 (4) (1993) 625–633.
[3] A. Ebrahimi, et al., Biological treatment of whey in an UASFF bioreactor followed a three-stage RBC, Chem. Ind. Chem. Eng. Q. 16 (2) (2010) 175–182.
[4] E. Zolghadr, et al., The role of membrane-based technologies in environmental treatment and reuse of produced water, Front. Environ. Sci. 9 (2021) 71.
[5] J. Rivas, A.R. Prazeres, F. Carvalho, Aerobic biodegradation of precoagulated cheese whey wastewater, J. Agric. Food Chem. 59 (6) (2011) 2511–2517.
[6] F. Carvalho, A.R. Prazeres, J. Rivas, Cheese whey wastewater: characterization and treatment, Sci. Total Environ. 445 (2013) 385–396.
[7] J.-C. Frigon, et al., The treatment of cheese whey wastewater by sequential anaerobic and aerobic steps in a single digester at pilot scale, Bioresour. Technol. 100 (18) (2009) 4156–4163.
[8] M. Amini, et al., Application of response surface methodology for simultaneous carbon and nitrogen (SND) removal from dairy wastewater in batch systems, Int. J. Environ. Stud. 69 (6) (2012) 962–986.
[9] A. Tawfik, M. Sobhey, M. Badawy, Treatment of a combined dairy and domestic wastewater in an up-flow anaerobic sludge blanket (UASB) reactor followed by activated sludge (AS system), Desalination 227 (1) (2008) 167–177.
[10] W. Chen, J. Liu, The possibility and applicability of coagulation-MBR hybrid system in reclamation of dairy wastewater, Desalination 285 (2012) 226–231.
[11] A. Suárez, T. Fidalgo, F.A. Riera, Recovery of dairy industry wastewaters by reverse osmosis. Production of boiler water, Separ. Purif. Technol. 133 (2014) 204–211.
[12] J.P. Kushwaha, V.C. Srivastava, I.D. Mall, Treatment of dairy wastewater by inorganic coagulants: parametric and disposal studies, Water Res. 44 (20) (2010) 5867–5874.

[13] S.F. Seyedpour, et al., Toward sustainable tackling of biofouling implications and improved performance of TFC FO membranes modified by Ag-MOF nanorods, ACS Appl. Mater. Interfaces 12 (34) (2020) 38285–38298.
[14] M. Pejman, et al., In situ Ag-MOF growth on pre-grafted zwitterions imparts outstanding antifouling properties to forward osmosis membranes, ACS Appl. Mater. Interfaces 12 (32) (2020) 36287–36300.
[15] A. Rahimpour, S. Madaeni, Y. Mansourpanah, High performance polyethersulfone UF membrane for manufacturing spiral wound module: preparation, morphology, performance, and chemical cleaning, Polym. Adv. Technol. 18 (5) (2007) 403–410.
[16] M. Hasheminejad, et al., Upstream and downstream strategies to economize biodiesel production, Bioresour. Technol. 102 (2) (2011) 461–468.
[17] S.S. Madaeni, Y. Mansourpanah, Screening membranes for COD removal from dilute wastewater, Desalination 197 (1–3) (2006) 23–32.
[18] A. Rahimpour, et al., The effect of heat treatment of PES and PVDF ultrafiltration membranes on morphology and performance for milk filtration, J. Membr. Sci. 330 (1–2) (2009) 189–204.
[19] E.S. Mansor, E.A. Ali, A. Shaban, Tight ultrafiltration polyethersulfone membrane for cheese whey wastewater treatment, Chem. Eng. J. 407 (2021), 127175.
[20] M. Kamali, et al., Sustainability considerations in membrane-based technologies for industrial effluents treatment, Chem. Eng. J. 368 (2019) 474–494.
[21] A. Cassano, et al., Fractionation of olive mill wastewaters by membrane separation techniques, J. Hazard Mater. 248 (2013) 185–193.
[22] R.K. Dereli, et al., Treatment of cheese whey by a cross-flow anaerobic membrane bioreactor: biological and filtration performance, Environ. Res. 168 (2019) 109–117.
[23] M. Paçal, N. Semerci, B. Çallı, Treatment of synthetic wastewater and cheese whey by the anaerobic dynamic membrane bioreactor, Environ. Sci. Pollut. Control Ser. 26 (32) (2019) 32942–32956.
[24] J. Ribera-Pi, et al., Anaerobic membrane bioreactor (AnMBR) for the treatment of cheese whey for the potential recovery of water and energy, Waste Biomass Valorization 11 (5) (2020) 1821–1835.
[25] L. Andrade, G. Motta, M. Amaral, Treatment of dairy wastewater with a membrane bioreactor, Braz. J. Chem. Eng. 30 (4) (2013) 759–770.
[26] B. Farizoglu, S. Uzuner, The investigation of dairy industry wastewater treatment in a biological high performance membrane system, Biochem. Eng. J. 57 (2011) 46–54.
[27] F. Meng, et al., Recent advances in membrane bioreactors (MBRs): membrane fouling and membrane material, Water Res. 43 (6) (2009) 1489–1512.
[28] P. Le-Clech, V. Chen, T.A. Fane, Fouling in membrane bioreactors used in wastewater treatment, J. Membr. Sci. 284 (1–2) (2006) 17–53.
[29] S.A. Deowan, et al., Novel low-fouling membrane bioreactor (MBR) for industrial wastewater treatment, J. Membr. Sci. 510 (2016) 524–532.
[30] J. Zhang, M. Zhang, K. Zhang, Fabrication of poly (ether sulfone)/poly (zinc acrylate) ultrafiltration membrane with anti-biofouling properties, J. Membr. Sci. 460 (2014) 18–24.
[31] S. Qiu, et al., Preparation and properties of functionalized carbon nanotube/PSF blend ultrafiltration membranes, J. Membr. Sci. 342 (1–2) (2009) 165–172.
[32] B. Chakrabarty, A. Ghoshal, M. Purkait, Preparation, characterization and performance studies of polysulfone membranes using PVP as an additive, J. Membr. Sci. 315 (1–2) (2008) 36–47.
[33] M.D. Firouzjaei, et al., Recent advances in functionalized polymer membranes for biofouling control and mitigation in forward osmosis, J. Membr. Sci. 596 (2020), 117604.
[34] M. Pejman, et al., Effective strategy for UV-mediated grafting of biocidal Ag-MOFs on polymeric membranes aimed at enhanced water ultrafiltration, Chem. Eng. J. (2021), 130704.
[35] D. Jang, et al., Effects of salinity on the characteristics of biomass and membrane fouling in membrane bioreactors, Bioresour. Technol. 141 (2013) 50–56.
[36] M.R. Esfahani, et al., Nanocomposite membranes for water separation and purification: fabrication, modification, and applications, Separ. Purif. Technol. 213 (2019) 465–499.
[37] M. Mozafari, et al., Facile Cu-BTC surface modification of thin chitosan film coated polyethersulfone membranes with improved antifouling properties for sustainable removal of manganese, J. Membr. Sci. 588 (2019), 117200.
[38] A. Zirehpour, et al., The impact of MOF feasibility to improve the desalination performance and antifouling properties of FO membranes, RSC Adv. 6 (2016) 70174–70185.
[39] J.B. Li, J.W. Zhu, M.S. Zheng, Morphologies and properties of poly (phthalazinone ether sulfone ketone) matrix ultrafiltration membranes with entrapped TiO2 nanoparticles, J. Appl. Polym. Sci. 103 (6) (2007) 3623–3629.
[40] H.S. Lee, et al., Polyamide thin-film nanofiltration membranes containing TiO2 nanoparticles, Desalination 219 (1–3) (2008) 48–56.
[41] M. Junaidi, et al., Fouling mitigation in humic acid ultrafiltration using polysulfone/SAPO-34 mixed matrix membrane, Water Sci. Technol. 67 (9) (2013) 2102–2109.
[42] J.-H. Choi, J. Jegal, W.-N. Kim, Fabrication and characterization of multi-walled carbon nanotubes/polymer blend membranes, J. Membr. Sci. 284 (1–2) (2006) 406–415.
[43] V. Vatanpour, et al., Boehmite nanoparticles as a new nanofiller for preparation of antifouling mixed matrix membranes, J. Membr. Sci. 401 (2012) 132–143.
[44] R. Pang, et al., Preparation and characterization of ZrO2/PES hybrid ultrafiltration membrane with uniform ZrO2 nanoparticles, Desalination 332 (1) (2014) 60–66.
[45] S. Liang, et al., A novel ZnO nanoparticle blended polyvinylidene fluoride membrane for anti-irreversible fouling, J. Membr. Sci. 394 (2012) 184–192.
[46] J. Hong, Y. He, Polyvinylidene fluoride ultrafiltration membrane blended with nano-ZnO particle for photo-catalysis self-cleaning, Desalination 332 (1) (2014) 67–75.
[47] A. Bottino, et al., Preparation and properties of novel organic–inorganic porous membranes, Separ. Purif. Technol. 22 (2001) 269–275.
[48] X. He, et al., In situ composite of nano SiO2–P (VDF-HFP) porous polymer electrolytes for Li-ion batteries, Electrochim. Acta 51 (6) (2005) 1069–1075.
[49] S. Zhao, et al., PSf/PANI nanocomposite membrane prepared by in situ blending of PSf and PANI/NMP, J. Membr. Sci. 376 (1–2) (2011) 83–95.
[50] L.-Y. Yu, et al., Preparation and characterization of PVDF–SiO2 composite hollow fiber UF membrane by sol–gel method, J. Membr. Sci. 337 (1–2) (2009) 257–265.
[51] L. Liu, C. Zhao, F. Yang, TiO2 and polyvinyl alcohol (PVA) coated polyester filter in bioreactor for wastewater treatment, Water Res. 46 (6) (2012) 1969–1978.
[52] V. Vatanpour, et al., TiO2 embedded mixed matrix PES nanocomposite membranes: influence of different sizes and types of nanoparticles on antifouling and performance, Desalination 292 (2012) 19–29.
[53] Z. Fan, et al., Performance improvement of polysulfone ultrafiltration membrane by blending with polyaniline nanofibers, J. Membr. Sci. 320 (1–2) (2008) 363–371.
[54] G.M. Shi, T. Yang, T.S. Chung, Polybenzimidazole (PBI)/zeolitic imidazolate frameworks (ZIF-8) mixed matrix membranes for pervaporation dehydration of alcohols, J. Membr. Sci. 415 (2012) 577–586.
[55] B. Zornoza, et al., Metal organic framework based mixed matrix membranes: an increasingly important field of research with a large application potential, Microporous Mesoporous Mater. 166 (2013) 67–78.
[56] M.D. Firouzjaei, et al., Exploiting synergetic effects of graphene oxide and a silver-based metal–organic framework to enhance antifouling and anti-biofouling properties of thin-film nanocomposite membranes, ACS Appl. Mater. Interfaces 10 (49) (2018) 42967–42978.
[57] A. Rahimpour, et al., Simultaneous improvement of antimicrobial, antifouling, and transport properties of forward osmosis membranes with immobilized highly-compatible polyrhodanine nanoparticles, Environ. Sci. Technol. 52 (9) (2018) 5246–5258.
[58] M. Dadashi Firouzjaei, et al., A novel nanocomposite with superior antibacterial activity: a silver-based metal organic framework embellished with graphene oxide, Adv. Mater. Interfaces 1701365 (2018) 1–10.
[59] F.A.A. Mostafa Dadashi Firouzjaeia, C. Milad Rabbani Esfahania, Turnera Heath, Siamak Nejati, Experimental and molecular dynamics study on dye removal from water by a graphene oxide-copper-metal organic framework nanocomposite, J. Water Process Eng. (2020) 10.
[60] S.F. Seyedpour, et al., Tailoring the biocidal activity of novel silver-based metal azolate frameworks, ACS Sustain. Chem. Eng. 8 (20) (2020) 7588–7599.
[61] J.-Y. Lee, C.Y. Tang, F. Huo, Fabrication of porous matrix membrane (PMM) using metal-organic framework as green template for water treatment, Sci. Rep. 4 (2014) 3740.
[62] C. Echaide-Górriz, et al., MOF nanoparticles of MIL-68 (Al), MIL-101 (Cr) and ZIF-11 for thin film nanocomposite organic solvent nanofiltration membranes, RSC Adv. 6 (93) (2016) 90417–90426.
[63] A. Synytsya, et al., Fourier transform Raman and infrared spectroscopy of pectins, Carbohydr. Polym. 54 (1) (2003) 97–106.
[64] A.A.G. Saeed Khoshhal, * Mohsen Jahanshahi and a.M. Mohammadi, in: Study of the Temperature and Solvent Content Effects on the Structure of Cu–BTC Metal Organic Framework for Hydrogen Storage, royal society of chemistry, 2015, pp. 24758–24768.
[65] A. Rahimpour, S.S. Madaeni, Y. Mansourpanah, The effect of anionic, non-ionic and cationic surfactants on morphology and performance of polyethersulfone ultrafiltration membranes for milk concentration, J. Membr. Sci. 296 (1) (2007) 110–121.
[66] D. Nagaraju, et al., In situ growth of metal-organic frameworks on a porous ultrafiltration membrane for gas separation, J. Mater. Chem. 1 (31) (2013) 8828–8835.
[67] J. Huang, G. Arthanareeswaran, K. Zhang, Effect of silver loaded sodium zirconium phosphate (nanoAgZ) nanoparticles incorporation on PES membrane performance, Desalination 285 (2012) 100–107.
[68] Z.-X. Li, et al., Hierarchically flower-like N-doped porous carbon materials derived from an explosive 3-fold interpenetrating diamondoid copper metal–organic framework for a supercapacitor, Inorg. Chem. 55 (13) (2016) 6552–6562.
[69] M. Pejman, et al., Improved antifouling and antibacterial properties of forward osmosis membranes through surface modification with zwitterions and silver-based metal organic frameworks, J. Membr. Sci. 611 (2020), 118352.
[70] A. Zirehpour, et al., The impact of MOF feasibility to improve the desalination performance and antifouling properties of FO membranes, RSC Adv. 6 (74) (2016) 70174–70185.
[71] H. Sun, B. Tang, P. Wu, Development of hybrid ultrafiltration membranes with improved water separation properties using modified superhydrophilic metal–organic framework nanoparticles, ACS Appl. Mater. Interfaces 9 (25) (2017) 21473–21484.
[72] M.L. Lind, et al., Influence of zeolite crystal size on zeolite-polyamide thin film nanocomposite membranes, Langmuir 25 (17) (2009) 10139–10145.
[73] J. Ma, et al., Composite ultrafiltration membrane tailored by MOF@ GO with highly improved water purification performance, Chem. Eng. J. 313 (2017) 890–898.
[74] A. Reuvers, C. Smolders, Formation of membranes by means of immersion precipitation: Part II. the mechanism of formation of membranes prepared from the system cellulose acetate-acetone-water, J. Membr. Sci. 34 (1) (1987) 67–86.

[75] A. Zirehpour, et al., Mitigation of thin-film composite membrane biofouling via immobilizing nano-sized biocidal reservoirs in the membrane active layer, Environ. Sci. Technol. 51 (10) (2017) 5511–5522.
[76] L. Shen, et al., Preparation and characterization of ZnO/polyethersulfone (PES) hybrid membranes, Desalination 293 (2012) 21–29.
[77] F. Qu, et al., Ultrafiltration membrane fouling caused by extracellular organic matter (EOM) from Microcystis aeruginosa: effects of membrane pore size and surface hydrophobicity, J. Membr. Sci. 449 (2014) 58–66.
[78] S. Zhao, et al., Improving permeability and antifouling performance of polyethersulfone ultrafiltration membrane by incorporation of ZnO-DMF dispersion containing nano-ZnO and polyvinylpyrrolidone, J. Membr. Sci. 478 (2015) 105–116.
[79] A. Rahimpour, et al., Novel functionalized carbon nanotubes for improving the surface properties and performance of polyethersulfone (PES) membrane, Desalination 286 (2012) 99–107.
[80] A. Rahimpour, S.S. Madaeni, Y. Mansourpanah, Nano-porous polyethersulfone (PES) membranes modified by acrylic acid (AA) and 2-hydroxyethylmethacrylate (HEMA) as additives in the gelation media, J. Membr. Sci. 364 (1–2) (2010) 380–388.
[81] M. Mazani, et al., Cu-BTC Metal– organic framework modified membranes for landfill leachate treatment, Water 12 (1) (2020) 91.
[82] B. Das, et al., Recovery of whey proteins and lactose from dairy waste: a step towards green waste management, Process Saf. Environ. Protect. 101 (2016) 27–33.
[83] J. Lee, et al., Graphene oxide nanoplatelets composite membrane with hydrophilic and antifouling properties for wastewater treatment, J. Membr. Sci. 448 (2013) 223–230.
[84] T. Hwang, et al., Ultrafiltration using graphene oxide surface-embedded polysulfone membranes, Separ. Purif. Technol. 166 (2016) 41–47.
[85] S. Mokhtari, et al., Enhancing performance and surface antifouling properties of polysulfone ultrafiltration membranes with salicylate-alumoxane nanoparticles, Appl. Surf. Sci. 393 (2017) 93–102.
[86] Y. Yang, et al., The influence of nano-sized TiO2 fillers on the morphologies and properties of PSF UF membrane, J. Membr. Sci. 288 (1–2) (2007) 231–238.
[87] S.A. Aktij, A. Rahimpour, A. Figoli, Low content nano-polyrhodanine modified polysulfone membranes with superior properties and their performance for wastewater treatment, Environ. Sci.: Nano 4 (10) (2017) 2043–2054.
[88] F. Gholami, S. Zinadini, A.A. Zinatizadeh, Preparation of high performance CuBTC/PES ultrafiltration membrane for oily wastewater separation; A good strategy for advanced separation, J. Environ. Chem. Eng. 8 (6) (2020), 104482.